available at www.sciencedirect.com

ScienceDirect

journal homepage: www.intl.elsevierhealth.com/journals/dema

The viscoelastic behavior of dental adhesives: A nanoindentation study

Alireza Sadr[a,*], *Yasushi Shimada*[a], *Hongbing Lu*[b], *Junji Tagami*[a,c]

[a] *Cariology and Operative Dentistry, Department of Restorative Sciences, Graduate School, Tokyo Medical and Dental University, 1-5-45 Yushima, Bunkyo-ku, Tokyo 113-8549, Japan*

[b] *School of Mechanical and Aerospace Engineering, Oklahoma State University, Stillwater, OK 74078, USA*

[c] *Center of Excellence Program for Frontier Research on Molecular Destruction and Reconstruction of Tooth and Bone, Tokyo Medical and Dental University, 1-5-45 Yushima, Bunkyo-ku, Tokyo 113-8549, Japan*

ARTICLE INFO

Article history:
Received 7 December 2007
Received in revised form
15 April 2008
Accepted 8 May 2008

Keywords:
Dental adhesives
Bonding
Viscoelasticity
Nanoindentation
Young's modulus
Creep compliance
Resin polymer
Self-etch
Filled resin
Etch and rinse

ABSTRACT

Objectives. In order to predict the long-term performance of dental adhesives, it is necessary to understand their mechanical properties. The objective of this study was to use a new nanoindentation technique to characterize the in-plane linear viscoelastic properties of dental adhesive layers.

Methods. The dental adhesives used were Clearfil SE Bond (CSE) and Clearfil Tri-S Bond (CTS) by Kuraray Medical and Single Bond (SIB) and Single Bond Plus (SBP) by 3M ESPE. A thin film of each adhesive was made on a micro-glass slide, and was then tested on a nanoindenter system (ENT 1100, Elionix) with a Berkovich indenter at a constant loading rate of 0.1 mN/s up to a maximum load of 1.8 mN. The load–displacement data of the loading segment were fitted to a curve to find best fit parameters for a generalized Kelvin viscoelastic model, from which creep compliance and Young's modulus were calculated. The modulus results were compared to the values calculated by the nanoindentation device.

Results. The experimental data fitted well to the viscoelastic model for all materials ($R > 0.9999$). SIB and CTS showed higher creep compliance compared to SBP and CSE. The modulus values obtained using the model were 4.0, 2.6, 2.4 and 4.2 GPa for CSE, CTS, SIB and SBP, respectively. The nanoindentation default software designed for time-independent materials significantly overestimated the modulus values up to 2.5 times.

Conclusion. As generally expected for polymer materials, the adhesives tested showed time-dependent viscoelastic behavior. The mechanical evaluation techniques developed for time-independent materials ignore this behavior and may not be appropriate for dental adhesives.

1. Introduction

With the recent developments in adhesive dentistry, evaluating the properties of adhesive materials has received an increasing attention [1]. In order to predict the long-term success of an adhesive restoration, it is necessary to critically evaluate the stress and deformation of the components in the bonded complex including the dental substrate, the restorative materials and the interfaces [2], as well as interfacial sealing and biological aspects of the degradation process [3].

Several techniques have been introduced to evaluate the mechanical performance of resins. The time-dependent vis-

* *Corresponding author*. Tel.: +81 3 5803 5483; fax: +81 3 5803 0195.
E-mail address: alireza.ope@tmd.ac.jp (A. Sadr).

0109-5641/$ – see front matter © 2008 Academy of Dental Materials. Published by Elsevier Ltd. All rights reserved.
doi:10.1016/j.dental.2008.05.001

coelastic response was shown to be an important feature of both natural and many synthetic biomaterials [4]. While the viscoelastic behavior of restorative composite resins has been investigated and emphasized by several studies [4–7]; few studies have measured this behavior for adhesive resins; perhaps because the available conventional methods developed for the bulk materials cannot be applied on bonding resins, which should be characterized in the actual in-use thin form [8].

Nanoindentation allows the investigation of selected material properties on small amounts of materials, based on the load–displacement data of indentations on a submicron scale. Measurement of mechanical properties by nanoindentation has been suggested as advantageous over the conventional methods for its high resolution of force and accurate indent positioning [1,2,9]. This method has been used to measure the elastic modulus and hardness of the dental adhesives by some researchers [1,2,10], using traditional analyses of penetration data obtained from the unloading curve of the indentations by the default software of the device, such as the Oliver and Pharr method [9]. These methods are generally based on Sneddon's solution for the relationship between the load and displacement for an axisymmetric indenter indenting into a half-space composed of a linear elastic, isotropic and homogeneous material [11].

On the other hand, time-dependence is the rule rather than the exception for polymers, even at low temperatures (especially near the glass-transition temperature). Well-known viscoelastic models like the simple generalized Maxwell or Kelvin model or the more sophisticated functions of Kohlrausch–Williams–Watts (KWW) or Wiechert have been shown to successfully describe the behavior of these materials in wide time scales [4,12]. A considerable progress has been recently made on the measurement of viscoelastic properties such as creep compliance and Young's relaxation modulus of thin film polymers using nanoindentation [13,14].

The aim of this study was to characterize the in-plane linear viscoelastic properties of dental adhesive layers using a new technique developed for nanoindentation.

2. Theory

The equations used in this study for extracting the linear viscoelastic properties from nanoindentation data in the time domain are presented here. The Berkovich indenter attached to the nanoindentation device is considered to be a rigid conical indenter. Sneddon [11] derived the relationship between load and displacement for a rigid conical indenter indenting into an elastic material as

$$h^2 = \frac{\pi(1-\nu)\tan\alpha}{4G}P \tag{1}$$

where P is the load, h is the displacement, α is the angle between the cone indenter and the substrate surface, ν is the Poisson's ratio, and G is the shear modulus. When the material has linear viscoelastic characteristics, the contact area between the indenter and the material has a time-dependent behavior. That means the boundary between the indenter and the half-space is moving. For this time-varying boundary problem a hereditary integral operator was proposed to determine the time-dependent stresses and deformations [15]. Applying this technique to Eq. (1) leads to the following equation for time-dependent indentation depth in a linear viscoelastic material under a prescribed arbitrary indentation loading history of $P(t)$.

$$h^2(t) = \frac{\pi(1-\nu)\tan\alpha}{4}\int_0^t J(t-\xi)\left[\frac{dP(\xi)}{d\xi}\right]d\xi \tag{2}$$

where $J(t)$ is the creep compliance in shear at time t, and ξ a dummy time variable of integration.

On the other hand the creep compliance of a linear viscoelastic material as expressed by the generalized Kelvin model is

$$J(t) = J_0 + \sum_{i=1}^{N} J_i(1 - e^{-t/\tau_i}) \tag{3}$$

where J_0–J_i are the compliance numbers, and τ_i is the retardation time.

Under a ramp loading at a constant loading rate of ν_0, $P(t) = \nu_0 t$. Substituting Eq. (3) into (2) leads to

$$h^2(t) = \frac{1}{4}\pi(1-\nu)\tan\alpha\left[\left(J_0 + \sum_{i=1}^{N} J_i\right)P(t) - \sum_{i=1}^{N} J_i(\nu_0\tau_i)(1 - e^{-P(t)/\nu_0\tau_i})\right] \tag{4}$$

In case Eq. (4) is fitted to the load–displacement curve obtained from nanoindentation, all parameters, J_0, J_i ($i = 1,\ldots, N$) and τ_i can be obtained. The parameters can then be used to determine the creep compliance relation as in Eq. (3). Moreover, the obtained creep compliance $J(t)$ can be used to determine other viscoelastic functions, such as the uniaxial relaxation modulus $E(t)$, which can be determined through the following relation:

$$\int_0^t E(\tau)J(t-\tau)d\tau = 2(1+\nu)t \tag{5}$$

where the Poisson's ratio ν is constant ($\nu = 0.3$ in this study).

3. Materials and methods

Bonding resins of four adhesive systems were evaluated in the current study: two-step self-etch system Clearfil SE Bond (CSE), all-in-one self-etch system Clearfil Tri-S Bond (CTS) (by Kuraray Medical, Tokyo, Japan) and etch-and-rinse systems Single Bond (SIB) and Single Bond Plus (SBP) (by 3M ESPE, St. Paul, MN, USA). The composition of each bonding resin is shown in Table 1.

A drop of each adhesive resin was placed on a micro-glass slide and then air-blown for 5 s to spread on the glass and remove water or solvents in case where the adhesives contained water or solvents. Another micro-glass slide was placed on the top and pressed against the bottom slide to reach

Table 1 – Group abbreviations and compositions of the adhesives tested in this study

Group	Classification	Name	Lot	Manufacturer
CSE (Clearfil SE Bond)	Two-step self-etch	Bonding agent: MDP, Bis-GMA, HEMA, hydrophobic DMA, CQ, DET, silanated colloidal silica filler	00729A	Kuraray Medical, Tokyo, Japan
CTS (Clearfil Tri-S Bond)	All-in-one self-etch	Water, MDP, Bis-GMA, HEMA, hydrophobic DMA, CQ, ethyl alcohol, silanated colloidal silica filler	00021A	
SIB (Single Bond)	Two-step etch and rinse	Bis-GMA, DMA, HEMA, water, ethanol, PAA, photoinitiator	4KG	3M ESPE, St. Paul, MN, USA
SBP (Single Bond Plus)	Two-step etch and rinse	Bis-GMA, DMA, HEMA, water, ethanol, PAA, photoinitiator, silane-treated silica filler	6GU	

Bis-GMA: bis-phenol A diglycidylmethacrylate; HEMA: 2-hydroxyethyl methacrylate; MDP: 10-methacryloyloxydecyl dihydrogen phosphate; DMA: dimethacrylate; DET: *N*,*N*-diethanol *p*-toluidine; CQ: camphorquinone; PAA: polyalkenoic acid copolymer.

a film thickness of 10–30 μm. The resin was light cured for 10 s according to the manufacturer's recommendation, using a halogen light curing unit (Optilux 501, Kerr Demetron, Danbury, CT, USA). After the specimens were left in the room temperature (23 ± 1 °C) for 24 h, the micro-glass slide on top was removed. The resulting thin film of bonding resin polymer was then tested in a nanoindenter system (ENT 1100, Elionix, Tokyo, Japan) using a three-sided pyramid diamond Berkovich tip with an enclosed angle of 130° at a constant loading rate of 0.1 mN/s up to a maximum load of 1.8 mN. The temperature of the testing chamber was held constant at 27.5 °C and the specimens were isolated inside the chamber for half an hour before the indentation to reach thermal balance and avoid effects of variable temperature.

During the loading segment 20 load–displacement data points were recorded per second. Ten indentations were programmed and performed on each sample out of which one typical indentation data set, representative of the average value of these indentations, was chosen for the calculations.

The load–displacement curve obtained from the selected indentation was then fitted to determine the best fit parameters of compliance numbers ($J_0, J_1, \ldots, J_N$) and retardation times ($\tau_1, \ldots, \tau_N$) in Eq. (4) using the ordinary least squares fitting technique (correlation coefficient $R > 0.9999$).

The creep function $J(t)$ determined for each material was then converted to $E(t)$ based on Eq. (5). A numerical approach was carried out to solve the problem. The value observed at $t = 18$ s was considered as the Young's modulus of material.

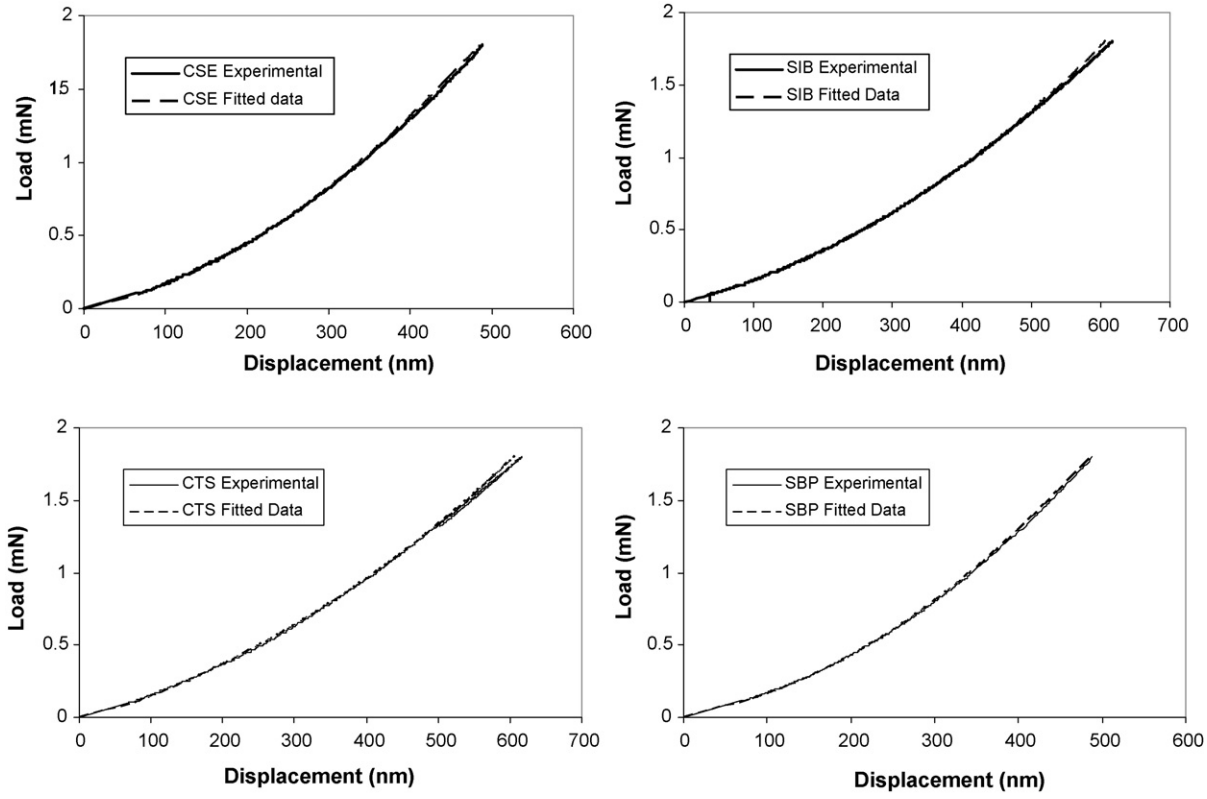

Fig. 1 – Load vs. displacement data for the loading segment in a typical indentation for each material. The continuous lines represent raw data from the nanoindentation experiment and the dashed lines show result of curve fitting. Good fitting was achieved for all materials in the selected loading range ($R > 0.9999$).

Table 2 – Hardness and Young's modulus values calculated by the methods discussed in the study

	Modulus based on the viscoelastic model (GPa)	Mean modulus by the indentation software (GPa)	Mean hardness at maximum load (MPa)
CSE	4.0	8.51	275
CTS	2.55	5.47	174
SIB	2.42	6.24	162
SBP	4.15	6.89	280

Kolmogorov Smirnov test indicated that there was a significant output difference between the two methods for calculation of Young's modulus ($p < 0.05$).

The values obtained for Young's modulus using the approach described above were finally compared to the means of values obtained from the conventional output from the default software of the computer attached to the nanoindentation device, using Kolmogorov Smirnov test.

Hardness values were obtained from the data at maximum load as previously described [8].

4. Results

The creep compliance formulas as obtained for each material are presented here. For all materials, favorable parameter values for Eq. (4) were found so that a good fit could be established for the experimental load–displacement data ($R > 0.9999$).

CSE $J(t) = 0.04(1 - e^{-10t}) + 0.331 (1 - e^{-t}) + 0.29(1 - e^{-0.1t})$

CTS $J(t) = 0.14 + 0.795(1 - e^{-0.25t}) + 0.173\ (1 - e^{-0.025t})$

SIB $J(t) = 0.393(1 - e^{-t}) + 0.485 (1 - e^{-0.22t}) + 0.187(1 - e^{-0.047t}) + 0.046 (1 - e^{-0.01t})$

SBP $J(t) = 0.032 + 0.377(1 - e^{-t}) + 0.228 (1 - e^{-0.1t}) + 0.0264(1 - e^{-0.01t})$

The load–displacement curve from the experiment and the fitted model are displayed in Fig. 1. The curves corresponding to the $J(t)$ equations are shown in Fig. 2.

SIB and CTS showed higher creep compliance compared to CSE and SBP. The Young's modulus values obtained from viscoelastic model and outputs of the default nanoindentation software together with mean hardness values are listed in Table 2. SIB and CTS showed lower Young's modulus values compared to CSE and SBP. Kolmogorov Smirnov test on the difference between the observed distributions for the output of the two methods indicated that there was a significant difference between the two ($p < 0.05$).

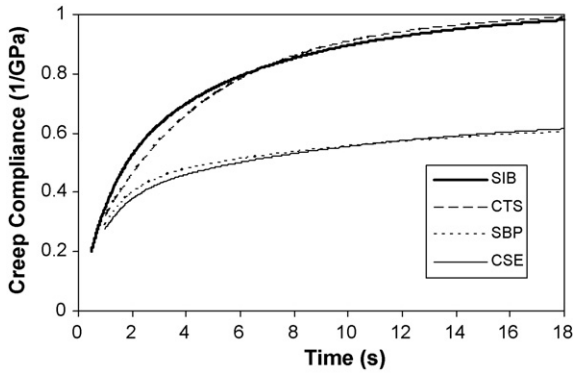

Fig. 2 – Creep compliance curves for each material based on the $J(t)$ relations given in the results.

5. Discussion

The modulus from the default software of the nanoindenter is determined based on a procedure derived from the Oliver and Pharr method [9], using the contact stiffness or slope of the tangent line obtained from fitting the initial part of load–displacement curve at the time of unloading and the contact area measured at the maximum nanoindentation load. While the method has been very effective and robust for elastic–plastic materials (without time-dependency), measurements on viscoelastic materials using this method have experienced problems [11]. The method tends to significantly overestimate the Young's modulus for a viscoelastic material such as polymer. The major reason is that during unloading, the displacement does not follow closely with the decreased load (as in the case for an elastic–plastic materials), due to prior increasing of the applied nanoindentation load and the memory effect of the time-dependent material. As a result, even though the load decreases during initial unloading, the displacement does not decrease at the same pace as the force, and sometimes could even increase during this initial stage, causing some high unloading slope or even a negative slope, as shown in Fig. 3., leading to the output of higher modulus than the actual value [14,16].

To take advantage of nanoindentation technique while avoiding the complications associated with the unloading curve, researchers have followed different approaches. A new method was employed in a previous study to evaluate the creep and stress exponent of the adhesives, holding the load constant for a period of time prior to unloading. It was speculated that the results were useful to predict the flaw resistance of the filled adhesive resin matrix [8]. Also, by modeling the instrument as a damped harmonic oscillator, it was possible to calculate the values of stiffness and modulus throughout the loading curve [13].

The generalized Kelvin model used in this study fitted well to the experimental load–displacement data for all materials within the selected loading history of the nanoindentation experiment, indicating the suitability of the linear viscoelastic model for the data in this loading range. The Young's relaxation modulus curves in the current study were calculated by conversion of the creep data to Eq. (5). Even though the method is prone to errors particularly due to the scattering of nanoin-

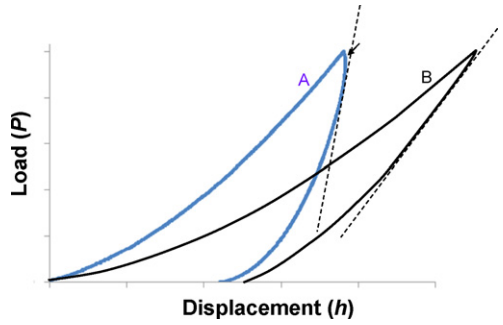

Fig. 3 – Nanoindentation load–displacement curves; (A) for SIB a viscoelastic material, and (B) for an elastic–plastic material. Black arrow shows a negative unloading slope at the very beginning of the unloading segment. Dashed lines are the slope of the upper portion of unloading curve or contact stiffness ($S = dP/dh$), from which the nanoindentation elastic modulus and plastic hardness are derived (Oliver and Pharr). The time-dependent behavior of (A) has led to an increased contact stiffness slope, which will eventually lead to overestimation of elastic modulus.

dentation data at early times, it was suggested that a very good agreement existed between the Young's modulus values obtained using this method and those of the conventional mechanical tests on bulk materials [14].

In the current study, the modulus values obtained using the viscoelastic model were all lower than those of the default nanoindentation output, and there was a significant difference between the two techniques. The previous nanoindentation studies have reported different values, up to four times higher than the value reported in the current study for CSE and SIB [1,17,18]. Values obtained for the Young's modulus using the conventional nanoindentation techniques, vary significantly depending on the loading rate [14] and the hold segment before unloading [2]; and this should explain the great variance of the previous results for the same material.

The materials in the current experiment were deposited on a glass-slide, in order to minimize the potential interfering factors in this experiment, such as dehydration of dental tissues and rough surface for the nano-scale test after polishing [10,19]. It was reported that for a soft film deposited on a hard substrate, the effect of substrate on the nanoindentation measurement could be neglected as long as the final depth of indentation was less than 20% of the film thickness [20,21]. In this study, the film thickness of adhesive resins polymerized on a glass-slide was over 10 μm, and the depth of indentations was always less than 700 nm; thus, the effect of substrate can be disregarded. Moreover, it has been suggested that the size, composition and distribution of filler particles in the resin exerted variation in the nanoindentation results [22]; results of the pilot investigations and previous studies [8,19] suggested that the fillers in adhesive materials used were of size and distribution attributes that had negligible effect on the data scatter among indentation points located within the matrix.

Selection of the four different materials was made in a manner to probe the effects of compositional differences between each two adhesives produced by the same manufacturer. CSE has been known as an established two-step self-etching primer bonding system [3,8,19]. While the primer agent of this material incorporates water and solvent, the bonding agent contains no such ingredients. On the other hand, CTS is an all-in-one bonding system with a composition similar to that of a hydrophilic combination of primer and bonding agents of Clearfil SE Bond. A comparison of the results obtained for the two materials imply that CTS bond has lower modulus of elasticity, lower hardness and higher creep compliance, than those of CSE.

In a polymer matrix, the chemical links established by cross-linking between molecular chains [23] and monomer conversion [5] increase the resistance to plastic flow and creep. It has been demonstrated that residual solvent in adhesive resins can significantly affect the degree of conversion [24]. It should be noted that, with regard to the sensitivity of the experimental nanoindentation technique and in order to obtain a homogenous film, only the bonding agent of CSE was polymerized instead of a mixture of the two agents. It has been demonstrated that clinically, high mechanical properties of CSE can be achieved when the primer is air-blown well and deprived of non-polymerizable components before the bonding agent is applied [8]. Moreover, in a clinical setup, the mineral components of dental substrate may neutralize the acidity of the self-etching systems and influence the polymerization efficacy [25], thus the properties of CTS in this experiment is likely to differ from those in clinical situations.

The proximity of the results obtained for CSE and SBP is probably due to their compositional analogy, indicating that from a mechanical point of view they may be similar. Moreover, SIB and SBP are materials with similar compositions, other than that SBP contain a 10% weight fraction of surface treated 5-nm diameter filler particles according to the manufacturer. A comparison of the results for these materials confirms that filler addition has significantly contributed to the mechanical properties of SBP, increasing hardness, Young's modulus and creep resistance compared to SIB. The addition of nanofillers resulted in an improvement in creep resistance of structure, which was attributed to the dense network formed by the filler particles with small volume fraction and surface treatment that effectively restricted the mobility of matrix polymer chains [26].

It has been suggested that a sufficiently flexible resin layer could resist the polymerization shrinkage stress of the restorative composite, thus a low modulus adhesive resin may be preferred. However, this would be the case probably only when the resin is sufficiently cured and the matrix has no structural defects. A low Young's modulus value might meanwhile be the result of prematurely polymerized and weak structure that has a poor resistance against stress.

Plasticization of methacrylate-based resins is an unfavorable phenomenon often linked to their polarity and porosity, leading to the change of the mechanical properties of the polymers [27]. Such method as the nanoindentation technique presented in the current study should be useful to describe the long-term changes occurring in the actual bonding layer exposed to moisture, in mechanistic terms suitable for polymers.

The common laboratory bond-strength tests, where the applied force increases to high levels in a short-term until fracture ensues, describe the failure behavior of materials in terms of linear fracture mechanics. Under such loading, the mobility of the cross-linked polymer chains is so limited that the molecular rearrangement in the macroscopic form of the material yield is very restricted. However, the terms may not apply when smaller loads are extended or cyclically repeated over time and relaxation or creep phenomena occur [4]. Time-dependent effect may continue until the polymer borders the cohesive zone, where a small load is needed to initiate a crack. Studies on the effect of cyclic loading on the adhesives confirm that while a bonding agent may display high bond-strength in the laboratory at the base-line, the cyclic loading would result in a significant reduction of bond-strength [28,29], sometimes with limited or no micro-morphologically detectable defects [30]. It has also been suggested that the static creep can be relevant clinically; and thus a useful method for the investigation of the behavior of dental restorative materials [4,5]. Further research is necessary to investigate different aspects of the observed viscoelastic behavior of dental adhesives.

6. Conclusion

This work discussed a nanoindentation technique for the evaluation of mechanical properties of dental adhesives. A good fitting was achieved between the viscoelastic model and the experimental nanoindentation raw data in this study. Adhesive materials exhibit time-dependent creep and relaxation. The attributes depend on the composition of materials and are likely to affect laboratory results and clinical outcome and thus, should not be ignored.

Acknowledgements

Authors are thankful to Dr Vahid Ravaghi of Queen Mary, University of London for his advice on the statistical analyses. This study was generously supported by a grant from Centre of Excellence (COE) Program, FRMDRTB at Tokyo Medical and Dental University, Tokyo, Japan.

REFERENCES

[1] Takahashi A, Sato Y, Uno S, Pereira PN, Sano H. Effects of mechanical properties of adhesive resins on bond strength to dentin. Dent Mater 2002;18:263–8.
[2] Van Meerbeek B, Willems G, Celis JP, Roos JR, Braem M, Lambrechts P, et al. Assessment by nano-indentation of the hardness and elasticity of the resin–dentin bonding area. J Dent Res 1993;72:1434–42.
[3] Yuan Y, Shimada Y, Ichinose S, Sadr A, Tagami J. Effects of dentin characteristics on interfacial nanoleakage. J Dent Res 2007;86:1001–6.
[4] Watts DC. Elastic moduli and visco-elastic relaxation. J Dent 1994;22:154–8.
[5] el Hejazi AA, Watts DC. Creep and visco-elastic recovery of cured and secondary-cured composites and resin-modified glass-ionomers. Dent Mater 1999;15:138–43.
[6] Braga RR, Ballester RY, Ferracane JL. Factors involved in the development of polymerization shrinkage stress in resin-composites: a systematic review. Dent Mater 2005;21:962–70.
[7] Papadogiannis Y, Lakes RS, Palaghias G, Helvatjoglu-Antoniades M, Papadogiannis D. Fatigue of packable dental composites. Dent Mater 2007;23:235–42.
[8] Sadr A, Shimada Y, Tagami J. Effects of solvent drying time on micro-shear bond strength and mechanical properties of two self-etching adhesive systems. Dent Mater 2007;23:1114–9.
[9] Oliver WC, Pharr GM. An improved technique for determining hardness and elastic-modulus using load and displacement sensing indentation experiments. J Mater Res 1992;7:1564–83.
[10] Hosoya Y. Hardness and elasticity of bonded carious and sound primary tooth dentin. J Dent 2006;34:164–71.
[11] Sneddon IN. The relation between load and penetration in the axisymmetric boussinesq problem for a punch of arbitrary profile. Int J Eng Sci 1965;3:47–57.
[12] Montgomery T, Shaw WJM. Viscoelastic models. In: Shaw MT, editor. Introduction to polymer viscoelasticity. 3rd ed. New York: Wiley–Interscience; 2005.
[13] Lin-Gibson S, Landis FA, Drzal PL. Combinatorial investigation of the structure-properties characterization of photopolymerized dimethacrylate networks. Biomaterials 2006;27:1711–7.
[14] Lu H, Wang B, Ma J, Huang G, Viswanathan H. Measurement of creep compliance of solid polymers by nanoindentation. Mech Time-Dependent Mater 2003;7:189–207.
[15] Lee EHRJ. The contact problem for viscoelastic bodies. J Appl Mech 1960;27:438.
[16] Hay JL, Pharr GM. Instrumented indentation testing. In: Kuhn H, Medlin D, editors. ASM handbook: mechanical testing and evaluation, vol. 8. OH: ASM International; 2000.
[17] Senawongse P, Harnirattisai C, Otsuki M, Tagami J. Effect of led light-curing time for the adhesive resin on the modulus of elasticity. Am J Dent 2007;20:139–41.
[18] Yamauti M, Nikaido T, Ikeda M, Otsuki M, Tagami J. Microhardness and young's modulus of a bonding resin cured with different curing units. Dent Mater J 2004;23:457–66.
[19] Sadr A, Ghasemi A, Shimada Y, Tagami J. Effects of storage time and temperature on the properties of two self-etching systems. J Dent 2007;35:218–25.
[20] Tsui TY, Pharr GM. Substrate effects on nanoindentation mechanical property measurement of soft films on hard substrates. J Mater Res 1999;14:292–301.
[21] Bhattacharya AK, Nix WD. Finite-element simulation of indentation experiments. Int J Solids Struct 1988;24:881–91.
[22] Drummond JL. Nanoindentation of dental composites. J Biomed Mater Res B: Appl Biomater 2006;78:27–34.
[23] Tai HJ. Structure and properties of poly(vinyl chloride)-triallyl cyanurate plastisols. Polym Eng Sci 2001;41:998–1006.
[24] Dickens SH, Cho BH. Interpretation of bond failure through conversion and residual solvent measurements and weibull analyses of flexural and microtensile bond strengths of bonding agents. Dent Mater 2005;21:354–64.
[25] Tay FR, Pashley DH. Aggressiveness of contemporary self-etching systems. I. Depth of penetration beyond dentin smear layers. Dent Mater 2001;17:296–308.
[26] Yang JL, Zhang Z, Schlarb AK, Friedrich K. On the characterization of tensile creep resistance of polyamide 66 nanocomposites. Part II. Modeling and prediction of long-term performance. Polymer 2006;47:6745–58.
[27] Ito S, Hashimoto M, Wadgaonkar B, Svizero N, Carvalho RM, Yiu C, et al. Effects of resin hydrophilicity on water sorption and changes in modulus of elasticity. Biomaterials 2005;26:6449–59.

[28] Nikaido T, Kunzelmann KH, Chen H, Ogata M, Harada N, Yamaguchi S, et al. Evaluation of thermal cycling and mechanical loading on bond strength of a self-etching primer system to dentin. Dent Mater 2002;18:269–75.
[29] Toledano M, Osorio R, Albaladejo A, Aguilera FS, Tay FR, Ferrari M. Effect of cyclic loading on the microtensile bond strengths of total-etch and self-etch adhesives. Oper Dent 2006;31:25–32.
[30] Frankenberger R, Pashley DH, Reich SM, Lohbauer U, Petschelt A, Tay FR. Characterisation of resin–dentine interfaces by compressive cyclic loading. Biomaterials 2005;26:2043–52.